A Computational Model Relating Structure and Reactivity in Enantioselective Oxidations of Secondary Alcohols by (−)-Sparteine−Pd^{II} Complexes

Robert J. Nielsen, Jason M. Keith, Brian M. Stoltz,*,‡ and William A. Goddard, III*

Contribution from the Materials and Process Simulation Center, Beckman Institute (139-74), and The Arnold and Mabel Beckman Laboratories of Chemical Synthesis, Division of Chemistry and Chemical Engineering, California Institute of Technology, Pasadena, California 91125

Received December 23, 2003; E-mail: wag@wag.caltech.edu; stoltz@caltech.edu

Abstract: The key interactions responsible for the unique reactivity of (−)-sparteine−PdX$_2$ complexes (X = chloride, acetate) in the enantioselective oxidation of secondary alcohols have been elucidated using quantum mechanics (B3LYP DFT with the PBF polarizable continuum solvent model). From examining many possible pathways, we find the mechanism involves: (1) substitution of the alcohol in place of an X-group, (2) deprotonation of the bound alcohol by the deposed anion and free sparteine, (3) β-hydride elimination through a four-coordinate transition state in which the second anion is displaced but tightly associated, (4) replacement of the ketone product with the associated anion. The enantioselectivities observed under base-rich reaction conditions follow directly from calculated energies of diastereomeric β-hydride elimination transition states incorporating (R) and (S) substrates. This relationship reveals an important role of the anion, namely to communicate the steric interaction of the ligand on one side of the Pd^{II} square plane and the substrate on the other side. When no anion is included, no enantioselectivity is predicted. Locating these transition states in different solvents shows that higher dielectrics stabilize the charge separation between the anion and metal and draw the anion farther into solution. Thus, the solvent influences the barrier height (rate) and selectivity of the oxidation.

Introduction

Recent examples of alcohol oxidations by Pd^{II} complexes and molecular oxygen, in the absence of copper cocatalysts, demonstrate increasing efficiency and selectivity. Generally, the metal (ligated to sp^2 [1−3] or sp^3 [4,5] nitrogen, DMSO,[6,7] and common anions) and a catalytic amount of excess base enable the dehydrogenation of an organic substrate by O$_2$, producing water or hydrogen peroxide. A subset of these reactions is the enantioselective oxidation of secondary alcohols to ketones by a (−)-sparteine−PdX$_2$ catalyst (X = Cl, OAc), generating primarily H$_2$O$_2$. Sparteine, an asymmetric natural product able to coordinate to Pd by two sp^3-nitrogen lone pairs, has engendered relative rates between (R) and (S) enantiomers of model aryl substrates of up to 47:1.[4,5] It has also proven useful in the synthesis of biologically important molecules.[8,9] The aim

Scheme 1
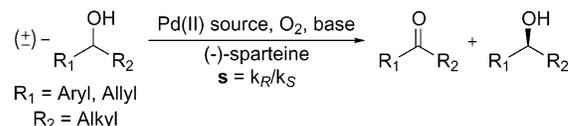
of this work is to trace the observed characteristics of this catalyst, and less effective ones, to their microscopic causes.

Previous studies by the Stoltz[4] and Sigman[5] groups have shown that an array of natural and synthetic ligands exhibit a wide range of reaction rate and selectivity in kinetic resolutions. Also, systematic variations in the reactivity of the (−)-sparteine−PdX$_2$ complexes as a function of substrate have been mapped.[10] Basic additives such as Cs$_2$CO$_3$ accelerate turnover,[11] presumably by aiding the deprotonation of the alcohol. A recent solvent screen[12] has shown chloroform offers rates and selectivites exceeding those previously measured in toluene. We used the specific kinetic data to guide our investigations, which in turn have revealed the atomistic factors that must be present to allow a ligand's potential selectivity to evidence itself. Using 1-phenylethanol as a representative substrate, we examined the mechanism by which (−)-sparteine−PdCl$_2$ functions. Then the consequences of changing anions and solvents were studied. The details of the methods are presented in section 2. The

‡ The Arnold and Mabel Beckman Laboratories of Chemical Synthesis, Division of Chemistry and Chemical Engineering.

(1) Nishimura, T.; Onoue, T.; Ohe, K.; Uemura, S. *J. Org. Chem.* **1999**, *64*, 6750.
(2) ten Brink, G.-J.; Arends, I. W. C. E.; Sheldon, R. A. *Science* **2000**, *287*, 1636.
(3) Steinhoff, B. A.; Stahl, S. S. *Org. Lett.* **2002**, *4*, 4179.
(4) Ferreira, E. M.; Stoltz, B. M. *J. Am. Chem. Soc.* **2001**, *123*, 7725.
(5) Jensen, D. R.; Pugsley, J. S.; Sigman, M. S. *J. Am. Chem. Soc.* **2001**, *123*, 7475.
(6) Peterson, K. P.; Larock, R. C. *J. Org. Chem.* **1998**, *63*, 3185.
(7) Steinhoff, B. A.; Fix, S. R.; Stahl, S. S. *J. Am. Chem. Soc.* **2002**, *124*, 766.
(8) Ali, I. S.; Sudalai, A. *Tetrahedron Lett.* **2002**, *43*, 5435.
(9) Caspi, D. D.; Ebner, D. C.; Bagdanoff, J. T.; Stoltz, B. M. *Adv. Synth. Catal.* **2004**, *346*, 185.

(10) Mueller, J. A.; Sigman, M. S. *J. Am. Chem. Soc.* **2003**, *125*, 7005.
(11) Bagdanoff, J. T.; Ferreira, E. M.; Stoltz, B. M. *Org. Lett.* **2003**, *5*, 835.
(12) Bagdanoff, J. T.; Stoltz, B. M. *Angew. Chem., Int. Ed.* **2004**, *43*, 353.

mechanism is described in section 3 while the selectivities are discussed in section 4. Further discussion is in section 5 with the conclusions in section 6.

2. Methods

Reported solution-phase energies (E_{sol}) are the sum of gas-phase electronic energies and solvation energies computed with the Poisson–Boltzmann reactive field method. The gas-phase energy is evaluated with the B3LYP[13] collection of gradient-corrected density functionals using a 6-31G**[14−16] basis set for light atoms (with diffuse functions added to Cl atoms and O atoms in acetate groups), the LACVP[17] relativistic effective core potential for Pd (which treats the 4s, 4p, 4d, and 5s electrons explicitly[18]), and the LAV3P[19] relativistic effective core potential for I (5s and 5p explicitly), augmented with a d-polarization shell as optimized by Höllwarth et al.[20] The solvation energy is the difference between solvated and unsolvated calculations performed with the described basis set sans diffuse functions. The solvent is represented as a polarizable continuum (with dielectric ϵ) surrounding the molecular complex at an interface constructed by combining atomic van der Waal radii with the effective probe radius of the solvent. Charges are allowed to develop on this interface according to the electrostatic potential of the solute and ϵ, then the polarized reaction field of the solvent acts back on the quantum mechanical description of the solute. The wave function of the complex is relaxed self-consistently with the reaction field to solve the Poisson–Boltzmann (PB) equations. Solvents were represented with the following parameters: toluene, $\epsilon = 2.379$, probe radius (r_p) = 2.762 Å; chloroform, $\epsilon = 4.806$, $r_p = 2.514$ Å; 1,2-dichloroethane, $\epsilon = 10.65$, $r_p = 2.513$ Å. Generally the gas-phase structures were used in the solvation calculations. In some cases (the relative energies in Table 1), the forces on the atoms from the reaction field of the solvent were used to optimize the structure of the solvated complex, allowing us to follow more precisely the effects of the dielectric. In such cases the relative energies are simply energy differences between solvent-optimized structures.

Stable intermediates are completely relaxed, while transition states are characterized by no interatomic forces and the presence of exactly one imaginary vibrational frequency. When a transition-state structure included a displaced anion, we often were not able to eliminate an imaginary frequency corresponding to the relative motion of the unbound fragments (in addition to the imaginary frequency of the reaction coordinate.) This probably results from numerical approximations in the methods which make it difficult to completely relax the very soft modes associated with such a loosely bound complex. However, such modes lead to very low force constants and cause only a negligible deviation in the transition-state energy.

3. Mechanism

General. Discussions of mechanisms for alcohol oxidations by palladium usually invoke a β-hydride elimination from a Pd–alkoxide formed by substrate coordination and deprotonation. Rather than study an assumed sequence of intermediates, the mechanism for the reaction of interest was determined by
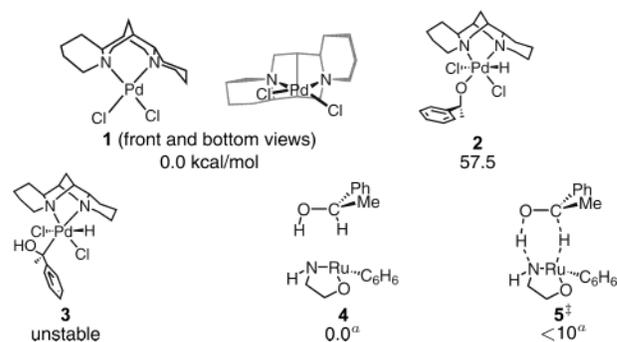
(13) Becke, A. D. *J. Chem. Phys.* **1993**, *98*, 5648.
(14) Hehre, W. J.; Ditchfield, R.; Pople, J. A. *J. Chem. Phys.* **1972**, *56*, 2257.
(15) Francl, M. M.; Pietro, W. J.; Hehre, W. J.; Binkley, J. S.; Gordon, M. S.; DeFrees, D. J.; Pople, J. A. *J. Chem. Phys.* **1982**, *77*, 3654.
(16) Hariharan, P. C.; Pople, J. A. *Theor. Chim. Acta* **1973**, *28*, 213.
(17) Hay, P. J.; Wadt, W. R. *J. Chem. Phys.* **1985**, *82*, 299.
(18) Basis functions for the valence electrons were contracted to double-ζ. The energies of key species were also evaluated with f-polarization functions on Pd. Since these functions served to change relative energies among intermediates by less than 0.2 kcal/mol, they were not employed.
(19) Wadt, W. R.; Hay, P. J. *J. Chem. Phys.* **1985**, *82*, 284.
(20) Höllwarth, A.; Böhme, M.; Dapprich, S.; Ehlers, A. W.; Gobbi, A.; Jonas, V.; Köhler, K. F.; Stegmann, R.; Veldkamp, A.; Frenking, G. *Chem. Phys. Lett.* **1993**, *208*, 137. Omitting d-functions on I yielded relative energies differing by over 2 kcal/mol.

Figure 1. ((−)-Sparteine)PdCl$_2$ and intermediates unlikely to participate in the oxidation mechanism. Energies (kcal/mol) for **1**−**3** are relative to **1** and include PB solvation by toluene ($\epsilon = 2.379$.) (a) From ref 22.

hypothesizing and testing many routes, using the predicted energetics to eliminate unlikely steps. 1-Phenylethanol, free sparteine, and (sparteine)PdCl$_2$ in toluene were taken as reactants (the reference state for energies.)

Paths involving oxidative addition to form Pd^{IV} species were found to be quite unfavorable. The products of O−H (**2**) and C−H (**3**) addition lie 58 kcal/mol above the reactants or are altogether unstable (Figure 1).

A slightly more feasible route comes by analogy to the ruthenium catalyst of Noyori et al.,[21] generated from RuCl$_2$-(η^6-benzene), β-amino alcohols, or *N*-tosyl-1,2-diamines, and strong base. That complex (represented by **4**) performs the same net transformation, *sec*-alcohol to ketone, in one pericyclic step, **5**‡. Yamakawa's calculations[22] suggest a barrier of less than 10 kcal/mol must be overcome when reacting methanol with the coordinatively unsaturated compound **4**. There are two striking differences, however, between the Ru^{II} and Pd^{II} complexes: the unsaturation of the Ru atom allows it to immediately accept hydride from the alcohol, and the amido nitrogen can accept a proton without significant geometric rearrangement. No analogous transition state was found involving the Pd^{II} compound, regardless of which base accepted the alcoholic proton: Cl$^-$ dissociating from Pd, a nitrogen of sparteine dissociating from Pd, or exogenous amine. The structures sampled during the search for a concerted mechanism lie more than 30 kcal/mol above the reactants, suggesting that the reaction on Pd consists of some combination of elementary steps.

Many possible paths involving coordination of alcohol, deprotonation, and C−H activation by β-hydride elimination are imaginable if one allows both Cl and sparteine to be displaced from the metal during the reaction. The lowest-energy route through these steps is plotted in Figure 2, along with some energetically competitive alternatives.[23] The alcohol enters the coordination sphere by associative substitution for a Cl$^-$ ion (**1**, **6**‡, **7**). The predicted barrier for this displacement ($\Delta E_{sol}^\ddagger = 3.8$ kcal/mol) is lowered by the Cl$^-$···H−OR hydrogen bond which forms as the substrate approaches. The free Cl$^-$ ion in **7** is not basic enough to deprotonate the bound alcohol alone, but the combination of Cl$^-$ and an exogenous sparteine molecule is. Deprotonation of the coordinated alcohol by free sparteine

(21) Hashiguchi, S.; Fujii, A.; Takehara, J.; Ikariya, T.; Noyori, R. *J. Am. Chem. Soc.* **1995**, *117*, 7562.
(22) Yamakawa, M.; Ito, H.; Noyori, R. *J. Am. Chem. Soc.* **2000**, *122*, 1466.
(23) Substitution of the alcohol for the other Cl, rotation around the alcohol's O−C bond, and use of (S)-1-phenylethanol lead to energy differences of up to 2 kcal/mol in structures **6**−**10**.
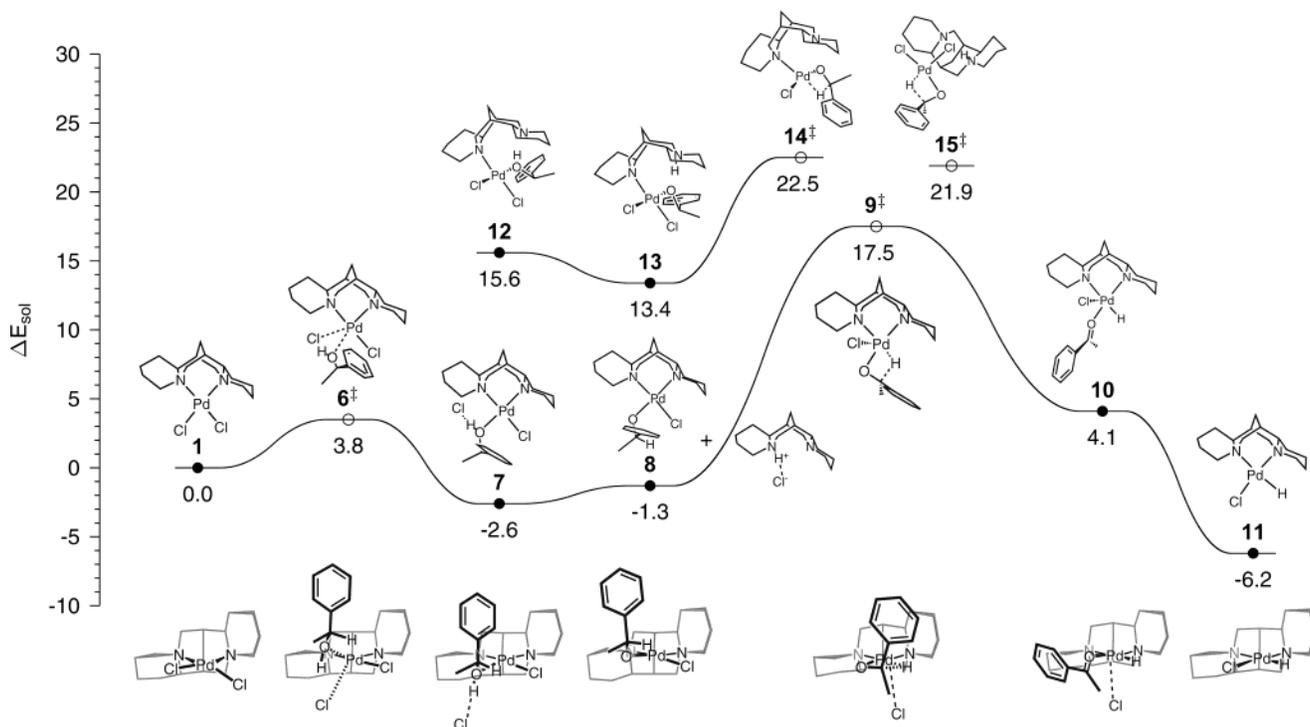
Figure 2. Mechanism for the oxidation of (*R*)-1-phenylethanol by ((−)-sparteine)PdCl₂. Energies (kcal/mol) are relative to **1** and include PB solvation by toluene ($\epsilon = 2.379$). Images are projections of the 3D structures, with corresponding bottom views aligned below.

has not been simulated (due to the large number of atoms and soft degrees of freedom associated with a second, unbound ligand), but the energetic barrier of this step is believed to be much smaller than that of the subsequent β-hydride elimination. (Such is the case for benzyl alcohol.[10]) The products of deprotonation in the models are the bound alkoxide **8** and a separate sparteine−H⁺Cl⁻ ion pair, which is predicted to be more stable than separate HCl and sparteine by $\Delta E_{sol} = 25.2$ kcal/mol. The relevance of structure **8** as an intermediate is supported by the recent X-ray characterization of an analogous species (in which the methyl group of the substrate is fluorinated) with the same structure.[24]

The alkoxide **8** is found to undergo β-hydride elimination through a four-coordinate transition state **9‡**, in which the remaining Cl atom is displaced to an axial, outer-sphere position 3.00 Å from Pd (Figure 3). The ketone produced (in **10**) is assumed to be easily replaced by the Cl atom, generating the more stable Pd−hydride complex **11**. A five-coordinate transition state was sought in which the Cl atom remains bound and the β-hydrogen approaches Pd from out of the square plane to replace the Pd−O bond. That such a structure could not be found is consistent with the fact that palladium's d-orbitals are correctly organized to allow a "2 + 2" metathesis reaction in the four-coordinate geometry **9‡**, but not in a five-coordinate geometry.[25] Attempts to find a five-coordinate transition state relaxed to the four-coordinate structure by displacing the Cl atom from the metal.

It is most intuitive to assume that the sparteine ligand imparts chirality to the metal center by remaining bidentate throughout the reaction and breaking the symmetry of the coordination sphere. Nonetheless, we also considered the dissociation of one
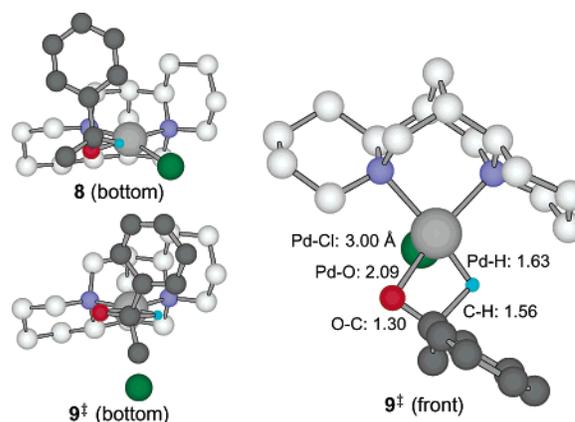
(24) Trend, R. M.; Stoltz, B. M. *J. Am. Chem. Soc.* **2004**, *126*, 4482.
(25) Steigerwald, M. L.; Goddard, W. A., III. *J. Am. Chem. Soc.* **1984**, *106*, 308.

Figure 3. Pd−alkoxide **8** and β-hydride elimination transition state **9‡**. Sparteine carbon atoms in light gray, chlorine in green.

or both N atoms of sparteine. A general result of the calculations is that the proximity of the nitrogen lone pairs and the bulk and rigidity of the ligand render it possible but unfavorable for sparteine to be bound to palladium by only one nitrogen. This is borne out by the peripheral structures in Figure 2. **12**−**14‡** belong to a mechanism featuring monodentate sparteine, and a low-energy β-hydride elimination transition state **15‡** was found in which both Cl atoms remain bound to Pd while protonated sparteine is present as a counterion. Besides being energetically less favorable than **9‡**, a mechanism including **14‡** or **15‡** likely suffers kinetically since sparteine must be removed from the metal. We speculate that sparteine possesses unusual kinetic stability; in addition to its chelation, its bulk hinders associative substitution mechanisms, and its rigidity hinders stepwise breaking of the N−Pd bonds. Finally, these alternate paths are not predicted to yield the enantioselectivities observed experimentally (vida infra).
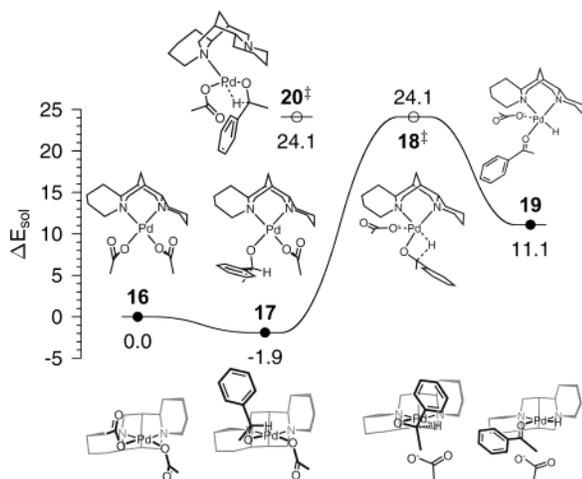
Figure 4. Abbreviated mechanism for the oxidation of (*R*)-1-phenylethanol by ((−)-sparteine)Pd(OAc)₂. Energies (kcal/mol) include PB solvation by toluene ($\epsilon = 2.379$.) Bottom views are aligned below.

Figure 5. β-Hydride elimination transition states incorporating chloride (**9‡**), acetate (**18‡**), and no anion (**21‡**), optimized in toluene. The anion nestles between the ligand and substrate, increasing the $C_{sparteine}-Pd-C_{methyl}$ angle θ.

The reoxidation of L_2PdXH species to L_2PdX_2 by O_2, a reaction general to many catalytic cycles besides the present one, warrants separate attention. This step is apparently not rate-limiting in oxidations featuring nitrogen-bound ligands under an oxygen atmosphere, and presently we find either of two suggestions plausible. O_2 may add across the Pd−H bond to produce a hydroperoxide complex, as proposed previously.[1,26,27] A hydroperoxide complex is expected to readily join the $\mathbf{1} \rightleftharpoons \mathbf{7} \rightleftharpoons \mathbf{8}$ equilibrium after protonation by a new alcohol or sparteine−H⁺Cl⁻ and liberation of H_2O_2. Alternatively, Stahl[28] has demonstrated that $(bc)Pd^0(\eta^2\text{-olefin})$ (bc = bathocuproine) yields $(bc)Pd^{II}X_2$ and H_2O_2 (via a stable $(bc)Pd^{II}(\eta^2\text{-peroxo})$ intermediate) upon attack by molecular oxygen and an acid, HX. If an analogous reduced species such as (sparteine)Pd⁰-(η^2-ketone) can be attained, perhaps by deprotonation of **10**, a similar mechanism should yield the starting material **1**.

The result of our studies is a mechanism that involves the same sequence of steps proposed by Mueller et al.,[29] whose observations of the same model reaction strongly support rate limitation by either deprotonation (at low sparteine loading) or β-hydride elimination (at high sparteine loading). Mueller found no reaction when no excess ligand was present, but as sparteine was added, the rate approached an asymptote at high loading. Also, when the α-hydrogen of 1-phenylethanol was replaced with deuterium, Mueller observed a kinetic isotope effect only under sparteine-saturated conditions. In light of these observations, we focus on the deprotonation (DP) and β-hydride elimination (βHE) elementary steps, their dependence on the catalyst's composition, and their control of the observed selectivity.

Chloride vs Acetate. The thermodynamics in Figure 2 suggest that deprotonation of **7** is driven by the concentration of reactants, not by an energetic force. As mentioned, excess sparteine (or other base) is required for reaction to occur using a dichloride Pd source. When ⁻OAc replaces Cl⁻ in the catalyst, however, the calculations predict that the ⁻OAc group displaced by th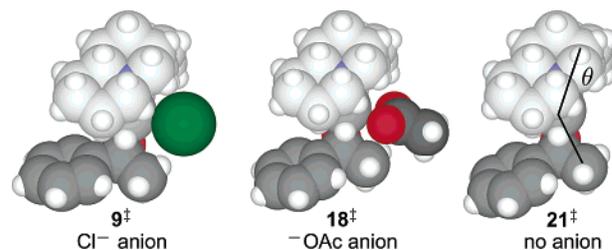e substrate deprotonates the alcohol directly, without the aid of an exogenous base (Figure 4). No stable analogue of structure **7** containing ⁻OAc was found; instead the proton hops from the alcohol to the acetate ion during the energy minimization. We find that the alkoxide **17** is more stable ($\Delta E_{sol} = -1.9$ kcal/mol) than the sparteine−Pd(OAc)₂ starting material **16**. (Again we consider that the acetic acid generated forms a hydrogen-bound complex with free sparteine, predicted to be only 10.2 kcal/mol more stable than separate acetic acid and sparteine.) Consequently we expect the alkoxide to play a larger role in the $\mathbf{16} \rightleftharpoons \mathbf{17}$ equilibrium when ⁻OAc replaces Cl⁻, leaving the overall reaction rate to be determined by the β-hydride elimination step at a lower concentration of base. Acetate's greater basicity is confirmed by the observation of modest reactivity when employing (sparteine)Pd(OAc)₂ with no added base.[10]

βHE transition-state structures and energies were found for 1-phenylethanol incorporating both Cl⁻ and ⁻OAc as the anion. They reveal the important role of X-groups in determining the selectivity and rate of elimination-limited reactions. The sample structures in Figure 5 illustrate that there is little direct interaction between the substrate and ligand. Instead, the temporarily displaced X-group lies between the two in a pocket lined by −CH groups of sparteine and the alcohol's methyl group. We believe that the role of the anion at this point in the mechanism is to communicate steric interactions between ligand and substrate, while not covalently bound but held in place by electrostatic forces. The $C_{sparteine}-Pd-C_{methyl}$ angle θ shown in Figure 5 increases from 135° in **21‡** to 139° in **18‡** to 146° in **9‡** to accommodate the counterions. By filling the space between the methyl group and ligand differently, the two anions present the same substrate with slightly different environments. The asymmetry of sparteine ensures that *R* and *S* alcohols face different combinations of steric interference as they pass through this transition state, hence the selectivity.

To validate the role of these diastereomeric transition-state structures their energies were used to predict enantioselectivities (s_{calc}) of reactions limited by β-hydride elimination using the method of the following section. A selectivity factor of $s_{calc} = 17.7$ is calculated for 1-phenylethanol in toluene at 60 °C when $X = Cl^-$, and $s_{calc} = 7.4$ at 80 °C in toluene and $s_{calc} = 14.9$ at 60 °C in 1,2-dichloroethane when $X = {}^-OAc$. Bagdanoff et al.[11] report $s_{exp} = 20.0$ at 60 °C using (norbornadiene)PdCl₂ as a palladium source. (This datum is interpreted here as representing the β-hydride elimination-controlled regime because of the excess base, Cs₂CO₃, present.) Starting with Pd(OAc)₂, Ferreira and Stoltz[4] report $s_{exp} = 8.8$ at 80 °C in toluene and Jensen et al.[5] report $s_{exp} = 13.0$ at 60 °C in dichloroethane.

(26) Hosokawa, T.; Murahashi, S.-I. *Acc. Chem. Res.* **1990**, *23*, 49.
(27) Takehira, K.; Hayakawa, T.; Orita, H. *Chem. Lett.* **1985**, 1835.
(28) Stahl, S. S.; Thorman, J. L.; Nelson, R. C.; Kozee, M. A. *J. Am. Chem. Soc.* **2001**, *123*, 7188.
(29) Mueller, J. A.; Jensen, D. R.; Sigman, M. S. *J. Am. Chem. Soc.* **2002**, *124*, 8202.

Table 1. Energetic and Structural Data of Diastereomeric β-Hydride Elimination Transition States

bidentate sparteine — R1, R2, S1, S2

Entry	Substrate / Anion	Solvent / Temp	E_{sol}^{a} ($\Delta E_{sol}^{\ddagger\,b}$), kcal/mol [R1]	C–H$_\beta$ (Å)	Pd···X^{d} (Å)	E_{sol} [R2]	C–H$_\beta$	Pd···X	E_{sol} [S1]	C–H$_\beta$	Pd···X	E_{sol} [S2]	C–H$_\beta$	Pd···X	s_{calc}^{c} / s_{exp}^{e}	$\Delta\Delta G_{eff,calc}$ / $\Delta\Delta G_{eff,exp}$
1	Ar = C$_6$H$_5$	toluene	0.0 (17.5)			1.73			2.82			2.03			17.7	1.9
	X = Cl$^-$	60°C		1.61	3.11		1.64	3.23		1.52	3.11		1.62	3.28	20.0^{f}	2.0
2	Ar = p-MeOC$_6$H$_4$	toluene	0.0 (16.6)			1.21			2.65			1.82			14.1	1.8
	X = Cl$^-$	60°C		1.58	3.25		1.61	3.28		1.48	3.12		1.59	3.31	14.9^{f}	1.8
3	Ar = p-FC$_6$H$_4$	toluene	0.0 (17.8)			1.18			2.36			1.63			10.3	1.5
	X = Cl$^-$	60°C		1.61	3.24		1.64	3.23		1.53	3.11		1.62	3.31	12.1^{f}	1.6
4	Ar = 2-Naphthyl	toluene	0.0 (15.7)			2.28			2.87			2.13			19.5	2.0
	X = Cl$^-$	60°C		1.59	3.11		1.64	3.23		1.52	3.11		1.62	3.29	15.8^{f}	1.8
5	Ar = C$_6$H$_5$	toluene	0.0 (24.1)			2.38			2.85			1.47			7.4	1.4
	X = $^-$OAc	80°C		1.64	2.83		1.65	2.84		1.59	2.65		1.66	2.90	8.8^{g}	1.5
6	Ar = C$_6$H$_5$	toluene	0.0 (—)			1.55			0.28			1.54			1.5	0.3
	None	60°C		1.50	—		1.55	—		1.50	—		1.55	—	NA	NA
7	Ar = C$_6$H$_5$	toluene	0.0 (14.5)			1.72			2.48			2.04			15.5	1.8
	X = I$^-$	60°C		1.56	3.42		1.61	3.82		1.53	3.93		1.61	3.64	NA	NA
8	Ar = C$_6$H$_5$	gas phase	0.0 (23.4)			1.54			3.55			1.64			12.5	1.7
	X = Cl$^-$	60°C		1.56	3.00		1.62	3.09		1.50	3.01		1.60	3.07	NA	NA
9	Ar = C$_6$H$_5$	chloroform	0.0 (14.6)			2.34			2.85			2.08			27.7	2.0
	X = Cl$^-$	23°C		1.62	3.22		1.67	3.32		1.56	3.23		1.64	3.31	30.7^{h}	2.0
10	Ar = C$_6$H$_5$	1,2-DCE	0.0 (26.5)			3.21			2.45			2.08			14.9	1.8
	X = $^-$OAc	60°C		1.64	3.05		1.66	3.00		1.58	3.21		1.66	3.00	13.0^{i}	1.7

monodentate sparteine — R3, R4, S3, S4

Entry	Substrate / Anion	Solvent / Temp	[R3]	C–H$_\beta$	Pd···X	[R4]	C–H$_\beta$	Pd···X	[S3]	C–H$_\beta$	Pd···X	[S4]	C–H$_\beta$	Pd···X	s	$\Delta\Delta G$
11	Ar = C$_6$H$_5$	toluene	0.60 (24.7)			0.07			1.23			0.0			1.1	0.1
	X = $^-$OAc	60°C		1.58	2.08		1.58	2.08		1.61	2.09		1.60	2.08	NA	NA

^{a} Relative to lowest-energy isomer. ^{b} Activation energy relative to reactants. ^{c} From eq 1. ^{d} When X = $^-$OAc, distance to nearest O atom. ^{e} Data best representing elimination-determined selectivities (i.e. base-rich reaction conditions) is used for comparison. ^{f} From ref 11. ^{g} From ref 4. ^{h} From ref 12. ^{i} From ref 5.

To further emphasize the anion's role in the β-hydride elimination step, transition states were found for (*R*)- and (*S*)-1-phenylethanol with no anion present. The separation of charge implied by removing the anion from the resulting cationic complex (e.g., **21**‡ in Figure 5) is energetically unrealistic in a low-dielectric medium such as toluene. Higher elimination barriers ($\Delta E_{sol}^{\ddagger}$ = 36.4 kcal/mol relative to reactants) are predicted when Cl$^-$ is solvated separately than when Cl$^-$ is allowed to remain close to the reaction center. More striking is that practically no discrimination between enantiomers is predicted (s_{calc} = 1.5), suggesting no selectivity would be observed if the anion were not present between the ligand and substrate to amplify it.

4. Selectivity

General. The enantioselectivity displayed by a catalyst/substrate pair is a convolution of the relative rates of the coordination (e.g. **1** → **7**), deprotonation (**7** → **8**) and β-hydride elimination (**8** → **10**) events. An algebraic expression for selectivity in terms of these rates (k_{Coord}, k_{DP}, $k_{\beta HE}$) and their associated equilibrium constants depends on one's choice of rate law and the conditions employed in the reaction and cannot be written down a priori. We find that selectivities observed in kinetic resolutions of racemic mixtures under base-rich conditions are accurately described by

$$s_{calc} = \frac{rate_R}{rate_S} = \frac{A_o \sum\limits_{R} \exp\left(-\dfrac{\Delta E_{sol}^{\ddagger}}{RT}\right)}{A_o \sum\limits_{S} \exp\left(-\dfrac{\Delta E_{sol}^{\ddagger}}{RT}\right)} \tag{1}$$

when $\Delta E_{sol}^{\ddagger}$ is the calculated energy of a βHE transition state relative to the reactants (Figure 6). Since the asymmetry of sparteine makes the two sites occupied by Cl atoms in the resting state incongruent, two βHE transition states exist for each enantiomer. Distinguished by which Cl atom is initially
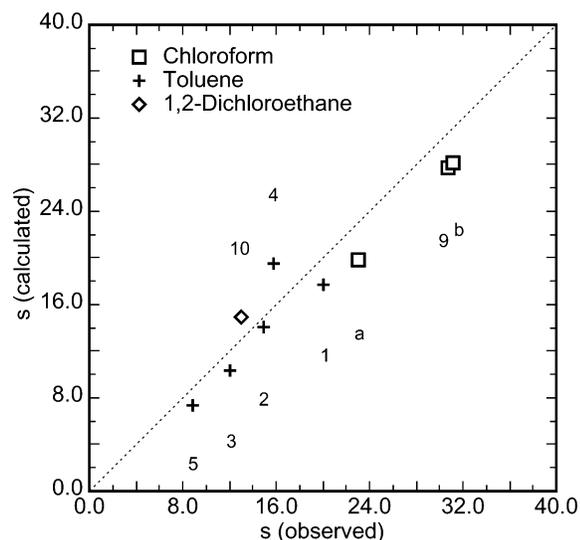
Figure 6. Calculated and experimental enantioselectivities. Labels denote corresponding entry in Table 1; a and b correspond to 1-(*p*-FC$_6$H$_4$)ethanol and 1-(2-naphthyl)ethanol, respectively, in chloroform at 23 °C, X = Cl$^-$.

displaced by the alcohol, we consider these two structures (e.g., R1 and R2 or S1 and S2 in Table 1) to belong to separate reaction pathways. (Four additional isomers, analogues of R1–S2, can be generated by swapping the methyl and aryl groups of the substrate so that the anion resides adjacent the aryl group instead of the methyl group. For 1-phenylethanol, the unfavorable interaction of the anion with the π-electrons of the aryl group causes the energies of these isomers to lie 2.5–4 kcal/mol above their analogues R1–S2, and these isomers were subsequently ignored.) Hence, the sums in eq 1 contain two terms per enantiomer. Equal prefactors A_o are assumed. By the same reasoning, experimental and calculated selectivities can be transformed into effective $\Delta\Delta G^{\ddagger}$'s (a measure of the degree to which a catalyst distinguishes between enantiomers) for a substrate/anion/solvent combination according to $\Delta\Delta G^{\ddagger}_{\text{eff}} = RT \ln(\mathbf{s})$. Using only sparteine as a ligand, Jensen et al. found that the selectivity between (*R*)- and (*S*)-1-phenylethanol ranged from 2.6 to 17.5, depending on their palladium source and reaction conditions.[5] Although the models only contain information regarding the substrate, X-group, solvent, and temperature, they are able to consistently reproduce the selectivities observed in elimination-limited reactions.

Equation 1 is consistent with an expression such as

$$\mathbf{s} = \frac{K_{\text{Coord,R}} K_{\text{DP,R}} k_{\beta\text{HE,R}}}{K_{\text{Coord,S}} K_{\text{DP,S}} k_{\beta\text{HE,S}}}$$

in which all steps prior to βHE reach preequilibrium. Expressions derived from more complex mechanisms cannot, however, be excluded. The selectivity observed in the DP-limited regime differs from that in βHE-limited reactions for a given catalyst and is likely described by $\mathbf{s} = K_{\text{Coord,R}} k_{\text{DP,R}} / K_{\text{Coord,S}} k_{\text{DP,S}}$. We focus on selectivity in the βHE-limited regime for two reasons. Barring a change in mechanism, new catalysts will achieve their highest rates under these conditions. Also, the βHE step may be more amenable to tuning with new ligands than deprotonation. An experimental combinatorial study[30] found that Pd complexes of both chiral and achiral ligands yielded functioning

(30) Jensen, D. R.; Sigman, M. S. *Org. Lett.* **2003**, *5*, 63.

catalysts in the presence of sparteine (acting only as a chiral deprotonating agent). Unfortunately, selectivities resulting from these asymmetric deprotonations were not improved over sparteine–Pd complexes operating in the βHE-limited regime.

Four βHE transition states were located for a sampling of substrates (1-substituted ethanols), solvents, and X-groups. The energetic and structural data collected in Table 1 show that configurations R1 and S2 provide the lowest-energy routes to the (*R*) and (*S*) substrates, respectively, although none of the four paths is negligible. We find the relative energies of the isomers are determined by three factors. First, transition-state energies are lower if the anion is displaced to the open face of the ligand (below Pd in Table 1) than if it moves to the occluded face (above Pd). The rightmost piperidine ring of sparteine (as drawn) disrupts the coordination sphere of Pd by interfering with both the adjacent equitorial site (e.g. the adjacent chlorine in **1** is bent out of the square plane) and upper axial site (e.g. the anion in structure S1). Whether the oxygen of the substrate bonds to the left or right site on Pd is another factor. In the favorable site (R1, S1), oxygen abuts the less obtrusive, leftmost piperidine ring. This effect is most clearly seen in entry 6, in which no anion is present to otherwise affect the relative energies. Third, as mentioned, displacing the anion toward the aryl group of the substrate requires more energy than displacing it toward the methyl group. By combining the favorable aspects of each of these factors, structure R1 provides (*R*) substrates with the fastest oxidation pathway.

Selectivity predictions based on the combination of *gas-phase* optimized transition-state energies and single-point solvation energies only qualitatively matched the experimental observations. In particular, this approach failed to capture the high selectivities observed when chloroform is used as solvent. This suggested that solvent-induced geometric relaxation plays a significant role in addition to electronic relaxation. Therefore, all structures R1 through S2 were optimized *within* the continuum solvent model, allowing the geometries and relative energies to more accurately reflect the action of the particular solvent.

Solvent Effects. Many organic solvents have proved competent for kinetic resolutions using sparteine–PdCl$_2$, with reactions in halomethanes excelling in both rate and selectivity.[12] Although the advantages associated with different solvents may also concern solubilities and the oxidation of the Pd–hydride intermediate, the effect of the dielectric on the βHE step is revealed by the evolution of the transition states in the different virtual solvents. The β-hydrogen displaces the remaining anion from its site as the C–H$_\beta$ bond breaks. Since breaking the polar Pd–X bond requires further separation of charge between the positively charged Pd center and the anion, it follows that a medium of increased dielectric strength should facilitate the process. The activation energies calculated for (*R*)-1-phenylethanol (traversing state R1, X = Cl$^-$) in a vacuum, toluene (ϵ = 2.4), and chloroform (ϵ = 4.8) are 23.4, 17.5, and 14.6 kcal/mol, respectively. We find this trend to be general of all substrates. (When X = $^-$OAc, the predicted activation energies increase with the dielectric constant, but the sparteine–HOAc byproduct is responsible for reversal of this trend. Unlike the sparteine–H$^+$Cl$^-$ complex, the acetic acid complex formed during the deprotonation of the bound alcohol is not polar enough to generate a large solvation energy. Consequently,

reactants (**16**) are favored over later intermediates as the dielectric increases. However, the energy difference between the *alkoxide* and *β*HE states is decreased by increasing dielectric strength whether X = Cl⁻ or ⁻OAc.) That the solvent is stabilizing the charge separation is manifest in the increasing Mulliken population of the Cl⁻ ion: -0.65 |e⁻| in a vacuum, -0.74 |e⁻| in toluene, and -0.79 |e⁻| in chloroform (structures R1 of entries 8, 1, and 9).

The increase in reaction rate observed in chloroform (relative to toluene) is apparently also the primary factor responsible for the observed increase in selectivity. A facile kinetic resolution can be performed at lower temperatures, where a catalyst's discrimination between enantiomers (i.e., $\Delta\Delta G^{\ddagger}_{\text{eff}}$) leads to a higher selectivity factor. For example, Bagdanoff, using a dichloride catalyst and 1-phenylethanol, reported a selectivity of 20.0 in toluene[11] at 60 °C and 31 in chloroform[12] at 23 °C, suggesting the same $\Delta\Delta G^{\ddagger}_{\text{eff}}$ of 2.0 kcal/mol in each solvent. However, a second mechanism is also at work, by which the solvent influences $\Delta\Delta G^{\ddagger}_{\text{eff}}$'s directly. 1-(*p*-fluoro)phenylethanol exhibited a selectivity of 12.1 at 60 °C in toluene[11] and 23 at 23 °C in chloroform,[12] yielding disparate $\Delta\Delta G^{\ddagger}_{\text{eff}}$'s of 1.65 and 1.84 kcal/mol, respectively. (Both increases and decreases in $\Delta\Delta G^{\ddagger}_{\text{eff}}$ are observed among the substrates.) Although possibly due to a difference in the activation entropies of enantiomers, this more subtle effect may also be mediated by the response of the displaced anion to more polar solvents. Two trends regarding the anion are clear in the calculations. One is the aforementioned accumulation of charge allowed by higher dielectrics. The second is the increase in the Pd···X distance in transition states optimized in more polarizable media. (See entries 8, 1, and 9, or 5 and 10.) In stabilizing the forming dipole the solvent draws the charged species further into solution. Together, these two effects allow the solvent to influence the effective size and position of the X-group. Since the X-group is responsible for communicating steric interactions from ligand to substrate, it follows that the solvent's influence should extend to the discrimination between enantiomers. An additional selectivity prediction using dichloromethane as solvent (for 1-phenylethanol at 60 °C, X = Cl⁻, $\epsilon = 9.1$) yielded $s_{\text{calc}} = 13.1$. The *β*HE structures relaxed in this dielectric show that the chloride ion moves still farther from the palladium center, and this is likely the cause of the decrease in calculated selectivity from chloroform to dichloromethane. We propose that there is a critical dielectric constant above which (with the help of entropy) the anion would be solvated entirely separate from the cationic complex. For example, using a dielectric of 80.4 to represent water we find the separate ions Cl⁻ and **21**‡ have a slightly *lower* energy than the complex **9**‡. Were the reactants still soluble in so polar a medium, enantioselectivity would be lost.

Substrates and Anions. The oxidation rates of substituted benzylic alcohols in the presence of excess sparteine were observed to increase with the electron-donating strength of the substituent.[10] This was attributed to a rate-limiting *β*HE step in which negative charge is drawn from the alkoxide to the resulting Pd–hydride complex. Our calculations involving para-substituted 1-phenylethanols (entries 1−3) show the same behavior; that is, the activation energies $\Delta E^{\ddagger}_{\text{sol}}$ increase with the Hammett parameters of the substrates. In accordance with the Hammond Postulate, we find that transition-state structures

of less easily oxidized substrates are more product-like. For example, the C–H$_\beta$ bond being broken in each transition state incorporating 1-(*p*-fluoro)phenylethanol is at least 0.03 Å longer than the corresponding C–H$_\beta$ bond in 1-(*p*-methoxy)phenyl-ethanol.

To explore the properties of other counterions, chlorine was replaced with iodine in the model reaction, and the key energetics were calculated. The predicted selectivity ($s_{\text{calc}} = 15.5$ at 60 °C, entry 7) is no greater than that of the dichloride catalyst, but the activation energy of the lowest *β*HE transition state ($\Delta E^{\ddagger}_{\text{sol,I,R1}} = 14.5$ kcal/mol) is lower (cf $\Delta E^{\ddagger}_{\text{sol,Cl,R1}} = 17.5$). This reflects the ground-state destabilization of the initial (sparteine)PdI₂ complex; the crowding of sparteine and the large iodine atoms around Pd effectively weakens the Pd–X bonds which must be broken during the cycle. High activity can be translated into higher selectivity by operating at a lower temperature, as noted.

When X = ⁻OAc, *β*HE transition states incorporating monodentate sparteine (entry 11) are as energetically accessible as those with the ligand chelated (entry 5). In this geometry the ligand dominates the coordination sphere even less than when bidentate, and the variation in energy among the isomers (and hence the predicted selectivity) is correspondingly small. Still another group of isomers exists in which the oxygen of the substrate bonds trans to monodentate sparteine, but the activation energies associated with this geometry are 8 kcal/mol higher than those for the structures shown.

Thermodynamics. The discussion above relies on solution-phase energies rather than enthalpies or free energies. Accurate gas-phase thermodynamic properties for the various intermediates can be calculated by applying the appropriate formulas of statistical mechanics to frequency spectra derived from calculated (gas phase) Hessians. Solution-phase enthalpies are accessible from the gas-phase values by subtracting PV and including the calculated solvation energies. This assumes the six hindered translational and rotational modes still behave classically and contribute $^6/_2kT$ to the total energy and the vibrational frequencies do not change appreciably in solution. In this manner solution-phase enthalpies H_{sol} at 298 K were calculated for the model reaction. This yielded: reactants (**1**), 0.0 kcal/mol; substitution transition state (**6**‡), 5.2; alcohol complex (**7**), −1.1; alkoxide complex (**8**), 1.3; and *β*HE transition state (**9**‡), 16.2. (The last value can be compared to the activation enthalpy of 16.8 kcal/mol measured by Mueller and Sigman[10] using an Eyring plot from 30 to 65 °C.) Since the "reactants" state is composed of three separate molecules (alcohol, sparteine–PdCl₂, and free sparteine) and subsequent stages of the oxidation involve only two (Pd–substrate complex and sparteine–H⁺Cl⁻ complex), the *free energy* of the reactants will be even lower relative to that of the other intermediates because of their greater entropy. This explains the observation of a first-order dependence of reaction rate on substrate concentration under all conditions. As long as the reactants are lowest in free energy, increased alcohol concentration will drive more palladium from state **1** to states **7** and onward.

The relative solution-phase *enthalpies* of the *β*HE transition states incorporating 1-phenylethanol and chloride (entry 1) are 0.0 (R1), 1.7 (R2), 2.8 (S1), and 2.1 (S2). In general, we find that selectivity predictions based on solution-phase enthalpies yield qualitatively similar results to those based on energies but

Scheme 2
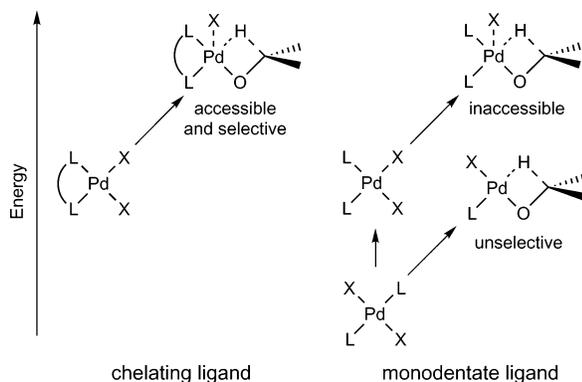
with more variation from the experimental measurements. The gas-phase entropies of the same four species are within 1 eu of one another, and for other substrates the variation is less than 5 eu. Therefore, we conclude that energy (or enthalpy) differences alone are sufficient to explain enantioselectivities derived from βHE. Thus, we rely on solution-phase energies, reaching the same conclusions and avoiding the assumptions associated with gas-phase Hessians.

5. Discussion

The ligands which have proved less selective than sparteine in kinetic resolutions of *sec*-alcohols are too numerous and complex to study individually. However, their structures and comparisons of the experimental and theoretical observations allow speculation regarding which motifs may be responsible for reaction rates and selectivities in current and future catalysts.

Brucine,[4] (+)-Troger's base, quinine (OTBS), and (*S*)-nicotine[5] each yielded higher rates than sparteine in the Pd-(OAc)$_2$-catalyzed oxidation of 1-phenylethanol under similar conditions. Their enantioselectivities, however, were unobservable or small. The former two in this group have only sp^3 N lone pairs available for bonding to Pd (neglecting oxygen atoms), while the latter two possess both sp^3 and sp^2 N atoms and O atoms. The geometries of all four dictate that they bond to Pd through only one N at a time. (*S,S*)-Ph-BOX,[5] (*S,S*)-Ph-PyBOX,[5,4] cinchonidine,[4] and others displayed no selectivity and lower rates than sparteine when tested. Possibly multidentate, these ligands provide either sp^2 (Ph-BOX, Ph-PyBOX) or both sp^2 and sp^3 N lone pairs. The chiral phosphine BINAP also showed rates similar to those of sparteine and no enantioselectivity.

Sparteine's rigid structure forces it to chelate in a cis, bidentate fashion, while L$_2$PdX$_2$-type compounds generally prefer a trans arrangement. If, for monodentate ligands, the alkoxide requires two of the four Pd sites during βHE, then the lowest-energy transition structure will have either the form LXPd(alkoxide) or L$_2$Pd(alkoxide). The former case is likey unselective for other ligands, as it is for sparteine. The latter case, which would require extra mechanistic steps to rearrange the ligands from a trans configuration, may be energetically inaccessible from the (more stable) trans resting state (Scheme 2), so it would seem only a catalyst with a cis resting state can lead to an accessible and selective βHE transition state.

Our work joins a number of increasingly quantitative calculations of the outcome of stereoselective reactions in solution and in proteins. Many algorithms have been applied to this problem, employing a variety of methods for the evaluation of energies (force fields,[31] DFT,[32] empirical correlations[33]) and structural models (explicit transition states or more abstract concepts[34]). Some factors which aid the reliability of predictions, however, are recurrent. Relative reaction rates often result from a flux of chiral or prochiral molecules through not only two transition states (e.g., (*R*) and (*S*)) but through a collection of diastereomeric states. A computational model should reflect this by averaging over an ensemble of all thermodynamically relevant reaction paths. Also, variations in the solvent-accessible surface of these isomeric transition states can contribute to or even determine[33] selectivity. A model of solvation is therefore helpful or necessary, depending upon the reaction in question.

6. Conclusions

The mechanism for oxidation of *sec*-alcohols by ((−)-sparteine)PdX$_2$ compounds begins with the facile substitution of an alcohol for an anion, followed by the deprotonation of the bound alcohol. Chloride is too weak a base to drive this step alone and requires free sparteine or a basic additive to form a Pd−alkoxide. Acetate and stronger bases can perform the deprotonation alone or in conjunction with sparteine at rates dependent on their basicity and concentration.

Once the ensuing β-hydride elimination step becomes rate-limiting, the enantioselectivity displayed by a catalyst in the presence of a racemic substrate is a function of the relative energies of an ensemble of diastereomeric βHE transition-state structures. The anion plays a critical role in these transition states by mediating the interaction between the otherwise estranged ligand and substrate. Solvents influence rate and selectivity during the elimination by accommodating an increase in charge on the anion. In addition to aiding the interpretation of existing results, the ability to compute activation energies and enantioselectivities provides a tool for screening new catalyst/substrate combinations.

Supporting Information Available: Gas phase and solvation energies and coordinates of numbered structures and representative structures from Table 1 and vibrational frequencies of transition states. This material is available free of charge via the Internet at http://pubs.acs.org.

JA031911M

(31) Norrby, P.-O.; Rasmussen, T.; Haller, J.; Strassner, T.; Houk, K. N. *J. Am. Chem. Soc.* **1999**, *121*, 10186 and references therein.
(32) Wiberg, K. B.; Bailey, W. F. *J. Am. Chem. Soc.* **2001**, *123*, 8231.
(33) Ke, T.; Wescott, C. R.; Klibanov, A. M. *J. Am. Chem. Soc.* **1996**, *118*, 3366.
(34) Lipkowitz, K. B.; Kozlowski, M. C. *Synlett* **2003**, 1547.
(35) Schrödinger, L. L. C. *Jaguar 4.0* and *Jaguar 5.0*; Portland, OR, 1991−2003.